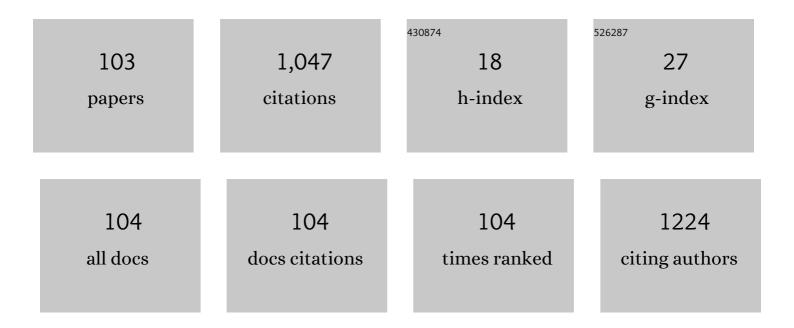
List of Publications by Year in descending order

Source: https://exaly.com/author-pdf/314543/publications.pdf Version: 2024-02-01



#	Article	IF	CITATIONS
1	Molecular speciation analysis of oxidized metal surfaces by TOF SIMS. Applied Surface Science, 2022, 577, 151855.	6.1	2
2	Characterisation of breast cancer molecular signature and treatment assessment with vibrational spectroscopy and chemometric approach. PLoS ONE, 2022, 17, e0264347.	2.5	3
3	Characterisation of Selected Materials in Medical Applications. Polymers, 2022, 14, 1526.	4.5	13
4	Development of novel spectroscopic and machine learning methods for the measurement of periodic changes in COVID-19 antibody level. Measurement: Journal of the International Measurement Confederation, 2022, 196, 111258.	5.0	21
5	Determination of idiopathic female infertility from infrared spectra of follicle fluid combined with gonadotrophin levels, multivariate analysis and machine learning methods. Photodiagnosis and Photodynamic Therapy, 2022, 38, 102883.	2.6	7
6	Remedial insight on ageing of glass through the study of ancient manâ€made artefacts. Archaeometry, 2021, 63, 312-326.	1.3	0
7	A Preliminary Study of FTIR Spectroscopy as a Potential Non-Invasive Screening Tool for Pediatric Precursor B Lymphoblastic Leukemia. Molecules, 2021, 26, 1174.	3.8	27
8	Spectroscopic evaluation of carcinogenesis in endometrial cancer. Scientific Reports, 2021, 11, 9079.	3.3	14
9	Probing calorimetric heat transfer phenomena in multi-nanophase substances: A case study of some over-stoichiometric nanoarsenicals. Thermochimica Acta, 2021, 701, 178955.	2.7	0
10	First identification of the effects of low frequency electromagnetic field on the micromolecular changes in adipose tissue-derived mesenchymal stem cells by fourier transform infrared spectroscopy. Journal of Medical Physics, 2021, 46, 253-262.	0.3	0
11	Raman and FTIR spectroscopy in determining the chemical changes in healthy brain tissues and glioblastoma tumor tissues. Spectrochimica Acta - Part A: Molecular and Biomolecular Spectroscopy, 2020, 225, 117526.	3.9	39
12	Simultaneous FTIR and Raman Spectroscopy in Endometrial Atypical Hyperplasia and Cancer. International Journal of Molecular Sciences, 2020, 21, 4828.	4.1	17
13	Microstructure and luminescent properties of Eu3+-activated MgGa2O4:Mn2+ ceramic phosphors. Journal of Advanced Ceramics, 2020, 9, 432-443.	17.4	23
14	The Spectroscopic Similarity between Breast Cancer Tissues and Lymph Nodes Obtained from Patients with and without Recurrence: A Preliminary Study. Molecules, 2020, 25, 3295.	3.8	4
15	Structure and antibacterial properties of Ag and N doped titanium dioxide coatings containing Ti2.85O4N phase, prepared by magnetron sputtering and annealing. Surface and Coatings Technology, 2020, 393, 125844.	4.8	11
16	Light-curing effects in acrylic-type dental nanocomposites probed by annihilating positrons: the case of densely monolith ĐCTA-3® restoratives. Applied Nanoscience (Switzerland), 2020, 10, 4791-4796.	3.1	0
17	Light-curing effects in acrylic-type dental nanocomposites probed by annihilating positrons: the case of loosely monolith Dipol® restoratives. Applied Nanoscience (Switzerland), 2020, 10, 4753-4758.	3.1	0
18	Depression as is Seen by Molecular Spectroscopy. Phospholipid- Protein Balance in Affective Disorders and Dementia. Current Molecular Medicine, 2020, 20, 484-487.	1.3	1

#	Article	IF	CITATIONS
19	Structure, Morphology, and Optical-Luminescence Properties of Eu3+- and Mn2+-Activated ZnGa2O4 and MgGa2O4 Ceramics. Springer Proceedings in Physics, 2020, , 363-378.	0.2	0
20	Classification of aggressive and classic mantle cell lymphomas using synchrotron Fourier Transform Infrared microspectroscopy. Scientific Reports, 2019, 9, 12857.	3.3	11
21	Identification of chemical changes in healthy breast tissue caused by chemotherapy using Raman and FTIR spectroscopy: A preliminary study. Infrared Physics and Technology, 2019, 102, 102989.	2.9	12
22	Predicting Ewing Sarcoma Treatment Outcome Using Infrared Spectroscopy and Machine Learning. Molecules, 2019, 24, 1075.	3.8	12
23	Spectroscopic identification of benign (follicular adenoma) and cancerous lesions (follicular) Tj ETQq1 1 0.7843 321-326.	14 rgBT /C 2.8	Overlock 10 T 15
24	The Role of a Thin Aluminum Film in the Reconstruction of Silicon's Near-Surface Layers. Lecture Notes in Mechanical Engineering, 2019, , 189-196.	0.4	0
25	FTIR Spectroscopy of Cerebrospinal Fluid Reveals Variations in the Lipid: Protein Ratio at Different Stages of Alzheimer's Disease. Journal of Alzheimer's Disease, 2019, 68, 281-293.	2.6	14
26	Tunable Color Filter Based on Optomechanical Plasmonic Device. , 2019, , .		0
27	Body Mass Index (BMI) and Infectious/Febrile Episodes in Children with Intermediate Risk Acute Lymphoblastic Leukemia (IR ALL). Nutrition and Cancer, 2019, 71, 701-707.	2.0	1
28	Effect of high-energy mechanical milling on the FSDP-related XRPD correlations in Se-rich glassy arsenic selenides. Journal of Physics and Chemistry of Solids, 2019, 124, 318-326.	4.0	12
29	Structure, morphology and optical-luminescence investigations of spinel ZnGa2O4 ceramics co-doped with Mn2+ and Eu3+ ions. Applied Nanoscience (Switzerland), 2019, 9, 907-915.	3.1	7
30	Free volume studies on mechanochemically milled β-As4S4 arsenical employing positron annihilation lifetime spectroscopy. Applied Nanoscience (Switzerland), 2019, 9, 647-656.	3.1	8
31	Silver nanoparticles deposited on calcium hydrogenphosphate – silver phosphate matrix; biological activity of the composite. Polish Journal of Chemical Technology, 2019, 21, 6-13.	0.5	2
32	Application of infrared spectroscopy for the identification of squamous cell carcinoma (lung) Tj ETQq0 0 0 rgBT	/Overlock	10
33	Surface oxidation of SnTe topological crystalline insulator. Applied Surface Science, 2018, 452, 134-140.	6.1	30
34	The classification of lung cancers and their degree of malignancy by FTIR, PCA-LDA analysis, and a physics-based computational model. Talanta, 2018, 186, 337-345.	5.5	61
35	Distinguishing Ewing sarcoma and osteomyelitis using FTIR spectroscopy. Scientific Reports, 2018, 8, 15081.	3.3	20
36	Luminescence and Nanopores in Spinel ZnGa2O4 Ceramics Doped with Mn2+ lons: Synthesis and		0

Properties of Nanomaterials., 2018,,.

#	Article	IF	CITATIONS
37	Role of Bi and Ga additives in the physical properties and structure of GeSe4-GeTe4 glasses. Materials Characterization, 2018, 142, 50-58.	4.4	2
38	Giant visible and infrared light attenuation effect in nanostructured narrow-bandgap glasses. Optics Letters, 2018, 43, 387.	3.3	6
39	Prediction of Ewing Sarcoma treatment outcome using attenuated tissue reflection FTIR tissue spectroscopy. Scientific Reports, 2018, 8, 12299.	3.3	7
40	Spectroscopic analysis of normal and neoplastic (WI-FTC) thyroid tissue. Spectrochimica Acta - Part A: Molecular and Biomolecular Spectroscopy, 2018, 204, 18-24.	3.9	21
41	Light-Curing Volumetric Shrinkage in Dimethacrylate-Based Dental Composites by Nanoindentation and PAL Study. Nanoscale Research Letters, 2017, 12, 75.	5.7	4
42	Application of infrared spectroscopy in the identification of Ewing sarcoma: A preliminary report. Infrared Physics and Technology, 2017, 83, 200-205.	2.9	15
43	Use of FTIR spectroscopy and PCA-LDC analysis to identify cancerous lesions within the human colon. Journal of Pharmaceutical and Biomedical Analysis, 2017, 134, 259-268.	2.8	45
44	Monitoring breast cancer treatment using a Fourier transform infrared spectroscopy-based computational model. Journal of Pharmaceutical and Biomedical Analysis, 2017, 143, 261-268.	2.8	29
45	Nanoscale Inhomogeneities Mapping in Ga-Modified Arsenic Selenide Glasses. Nanoscale Research Letters, 2017, 12, 88.	5.7	2
46	Fourier Transform Infrared (FTIR) spectroscopy of paraffin and deparafinnized bone tissue samples as a diagnostic tool for Ewing sarcoma of bones. Infrared Physics and Technology, 2017, 85, 364-371.	2.9	27
47	Verification of the effectiveness of the Fourier transform infrared spectroscopy computational model for colorectal cancer. Journal of Pharmaceutical and Biomedical Analysis, 2017, 145, 611-615.	2.8	13
48	The use of high-mass clusters to measure the TOF SIMS profiles of implanted bismuth. International Journal of Mass Spectrometry, 2017, 422, 143-145.	1.5	1
49	Nanostructurization effects in PVP-stabilized tetra-arsenic tetra-sulfide As4S4 nanocomposites. Materials Chemistry and Physics, 2017, 186, 251-260.	4.0	15
50	Optical properties of ZnCoO layers obtained by PLD method. Materials Science-Poland, 2017, 35, 878-884.	1.0	2
51	Mathematical modeling of elementary trapping-reduction processes in positron annihilation lifetime spectroscopy: methodology of Ps-to-positron trapping conversion. Journal of Physics: Conference Series, 2017, 936, 012049.	0.4	3
52	The Influence of Sonication and Silver Nanoparticles Doped on Viscoelastic Structure of Agarose Gel. Acta Physica Polonica A, 2017, 132, 152-154.	0.5	2
53	Comparing paraffined and deparaffinized breast cancer tissue samples and an analysis of Raman spectroscopy and infrared methods. Infrared Physics and Technology, 2016, 76, 217-226.	2.9	38
54	An out-of-specification element oxide found in the subsurface layer of Ni superalloys after annealing in air. Corrosion Science, 2016, 108, 205-208.	6.6	0

#	Article	IF	CITATIONS
55	Experimental Investigation of Electrical Conductivity and Permittivity of SC-TiO 2 -EG Nanofluids. Nanoscale Research Letters, 2016, 11, 375.	5.7	26
56	FPA-FTIR Microspectroscopy for Monitoring Chemotherapy Efficacy in Triple-Negative Breast Cancer. Scientific Reports, 2016, 6, 37333.	3.3	36
57	On the energetic criterion for destructive clustering of metallic nanoparticles in chalcogenide and oxide glassy matrices. Physica Status Solidi (B): Basic Research, 2016, 253, 494-498.	1.5	2
58	Role of electron-phonon interaction in the temperature dependence of the phonon mode frequency in II-VI compound alloys. Physica Status Solidi C: Current Topics in Solid State Physics, 2016, 13, 510-513.	0.8	0
59	Comparison of oxidation processes in binary selenides and tellurides. Surface and Interface Analysis, 2016, 48, 547-551.	1.8	6
60	Application of Raman Spectroscopy and Infrared Spectroscopy in the Identification of Breast Cancer. Applied Spectroscopy, 2016, 70, 251-263.	2.2	92
61	Destructive Clustering of Metal Nanoparticles in Chalcogenide and Oxide Glassy Matrices. Nanoscale Research Letters, 2016, 11, 34.	5.7	5
62	Characterization Of Oxide Layers Produced On The AISI 321 Stainless Steel After Annealing. Archives of Metallurgy and Materials, 2015, 60, 2327-2334.	0.6	2
63	Ga-modified As2Se3–Te glasses for active applications in IR photonics. Optical Materials, 2015, 46, 228-232.	3.6	25
64	Surface phenomena in a precipitation-hardenable nickel–chromium alloy during multiple heating/cooling. Thin Solid Films, 2015, 591, 311-315.	1.8	2
65	Influence of the electron-phonon interaction on the temperature dependence of the phonon mode frequency in the II-VI compound solid solutions. Journal of Applied Physics, 2015, 117, 025702.	2.5	2
66	Study of Ga incorporation in glassy arsenic selenides by high-resolution XPS and EXAFS. Journal of Chemical Physics, 2015, 142, 184501.	3.0	17
67	Changes of PbSnTe thin film thickness due to the oxidation by different methods. Thin Solid Films, 2015, 591, 346-350.	1.8	1
68	Pb–Te–O phase equilibrium diagram and the lead telluride thermal oxidation. Thermochimica Acta, 2014, 579, 64-69.	2.7	5
69	Quantitative imaging of diatoms by PeakForce atomic force microscopy. Surface and Interface Analysis, 2014, 46, 851-855.	1.8	2
70	Composition of PbTe oxides obtained by different methods. Materials Science in Semiconductor Processing, 2014, 21, 20-25.	4.0	1
71	Time-of-Flight Secondary Ion Mass Spectroscopy with Bismuth Primary Ions of Clean and Air-Exposed Surfaces of Tellurium. European Journal of Mass Spectrometry, 2014, 20, 429-436.	1.0	2
72	Reinterpretation of the Ga <scp>A</scp> s <scp>P</scp> farâ€infrared spectra within the framework of the Verleur and Barker model of the alloy phonon spectra. Physica Status Solidi (B): Basic Research, 2013, 250, 1614-1623.	1.5	8

#	Article	IF	CITATIONS
73	Restructuring of the phonon spectra of the MCT and MZT alloy at the Dirac point singularity. , 2011, , .		Ο
74	Ion distribution preferences in ternary crystals ZnxCd1â^'xTe, Zn1â^'xHgxTe and Cd1â^'xHgxTe. European Physical Journal B, 2011, 84, 183-195.	1.5	7
75	Additional and canonical phonon modes in <mml:math xmlns:mml="http://www.w3.org/1998/Math/MathML"</mml:math 		

#	Article	IF	CITATIONS
91	Phonon and vibrational spectra of hydrogenated CdTe. Journal of Applied Physics, 2006, 100, 013521.	2.5	21
92	Vibrational spectra of hydrogenated CdTe. Physica Status Solidi C: Current Topics in Solid State Physics, 2005, 2, 1147-1154.	0.8	14
93	Effect of band inversion on the phonon spectra of Hg1–xZnxTe and Hg1–xCdxTe semiconductor alloys. Physica Status Solidi C: Current Topics in Solid State Physics, 2004, 1, 2836-2839.	0.8	3
94	Magnetophonon resonance in Mn Cd Hg1â´'â´'Te and Zn Cd Hg1â´'â´'Te. Journal of Alloys and Compounds, 2004, 371, 103-106.	5.5	2
95	Manifestation of defects in phonon spectra of binary zinc-blende compounds. EPJ Applied Physics, 2004, 27, 321-324.	0.7	2
96	Determining MnxCdyHg1–x–yTe and ZnxCdyHg1–x–yTe material parametersby magnetophonon spectroscopy. Physica Status Solidi A, 2003, 195, 255-259.	1.7	0
97	<title>Determining of the material parameters of&lt;br&gt;Zn&lt;formula&gt;&lt;inf&gt;&lt;roman&gt;x&lt;/roman&gt;&lt;/inf&gt;&lt;/formula&gt;Cd&lt;formula&gt;&lt;inf&gt;&lt;roman&gt;y&lt;/roman&gt;&lt;/inf&gt;&lt;/formula&gt;H&lt;br&gt;by magnetophonon spectroscopy</title> . , 2001, 4412, 263.	g <formula< td=""><td>ı&gt;∢onf&gt;<rora< td=""></rora<></td></formula<>	ı>∢onf> <rora< td=""></rora<>
98	Investigation of the strain layers in multiple quantum wells by magnetophonon resonance. , 2001, 4413, 248.		1
99	Magnetophonon spectroscopy of Zn Cd Hg1â^'â^'Te. Physica B: Condensed Matter, 2001, 298, 457-461.	2.7	1
100	Magnetophonon resonance as method of controlling of the thermal stress in the multiple quantum wells. Materials Science & Engineering A: Structural Materials: Properties, Microstructure and Processing, 2000, 288, 138-141.	5.6	2
101	Multimode nature and magnetophonon resonance of quaternary solid solutions of zinc, cadmium, and mercury tellurides. Semiconductors, 1998, 32, 901-909.	0.5	3
102	Magnetotransport phenomena in multimode lattices. Journal of Physics Condensed Matter, 1998, 10, 8587-8610.	1.8	8
103	Influence of Temperature on Magnetophonon Resonances in Four-Component Solid Solution of ZnxCdyHg1â^'xâ^'yTe. Physica Status Solidi (B): Basic Research, 1995, 192, 121-127.	1.5	6